



HAL
open science

Multi-point Assessment of the Kinematics of Shocks (MAKOS): A Heliophysics Mission Concept Study. (Whitepaper #135 in the Decadal Survey for Solar and Space Physics (Heliophysics) 2024-2033.)

Katherine Goodrich, Lynn Iii, Steven Schwartz, Ian Cohen, Drew Turner, Phyllis Whittlesey, Amir Caspi, Randy Rose, Keith Smith, Robert Allen, et al.

► To cite this version:

Katherine Goodrich, Lynn Iii, Steven Schwartz, Ian Cohen, Drew Turner, et al.. Multi-point Assessment of the Kinematics of Shocks (MAKOS): A Heliophysics Mission Concept Study. (Whitepaper #135 in the Decadal Survey for Solar and Space Physics (Heliophysics) 2024-2033.). Bulletin of the American Astronomical Society, 2023, 55 (3), 10.3847/25c2cfcb.431a46a0 . hal-04289416

HAL Id: hal-04289416

<https://hal.science/hal-04289416v1>

Submitted on 9 Feb 2024

HAL is a multi-disciplinary open access archive for the deposit and dissemination of scientific research documents, whether they are published or not. The documents may come from teaching and research institutions in France or abroad, or from public or private research centers.

L'archive ouverte pluridisciplinaire **HAL**, est destinée au dépôt et à la diffusion de documents scientifiques de niveau recherche, publiés ou non, émanant des établissements d'enseignement et de recherche français ou étrangers, des laboratoires publics ou privés.



Distributed under a Creative Commons Attribution 4.0 International License



Multi-point Assessment of the Kinematics of Shocks (MAKOS): A Heliophysics Mission Concept Study

K. A. Goodrich¹, L. B. Wilson III², S. Schwartz³, I. J. Cohen⁴, D. L. Turner⁴, P. Whittlesey⁵,
A. Caspi⁶, R. Rose⁶, K. Smith⁶

Endorsed by:

R. Allen⁴, D. Burgess⁷, D. Caprioli⁸, P. Cassak¹, J. Eastwood⁹, J. Giacalone¹⁰, I. Gingell¹¹, C. Haggerty¹², J. Halekas¹³,
G. Hospodarsky¹³, G. Howes¹³, J. Juno¹⁴, Y. Khotyaintsev¹⁵, K. Klein¹⁰, H. Kucharek¹⁶, B. Lembège¹⁷, E. Lichko¹⁰,
T. Liu¹⁸, D. Malaspina³, M. F. Marcucci¹⁹, C. Mazelle²⁰, K. Meziane²¹, F. Plaschke²², A. Retino²³, C. T. Russell¹⁸,
E. Scime¹, D. Sibeck², M. Stevens²⁴, J. TenBarge²⁵, I. Vasko⁵, L. Wang²⁶, S. Wang²⁷, H. Zhang²⁸

¹West Virginia University, ²NASA Goddard Space Flight Center, ³University of Colorado Boulder, ⁴The Johns Hopkins University Applied Physics Laboratory, ⁵University of California Berkeley, ⁶Southwest Research Institute, ⁷Queen Mary University of London, ⁸University of Chicago, ⁹Imperial College London, ¹⁰University of Arizona, ¹¹University of Southampton, ¹²University of Hawaii, ¹³University of Iowa, ¹⁴Princeton Plasma Physics Laboratory, ¹⁵Swedish Institute of Space Physics, ¹⁶University of New Hampshire, ¹⁷LATMOS - CNRS- IPSL-UVSQ, ¹⁸University of California Los Angeles, ¹⁹INAF, ²⁰IRAP CNRS University of Toulouse CNES, ²¹University of New Brunswick, ²²IGEP, TU Braunschweig, ²³LPP, CNRS, Sorbonne Université, Université Paris Saclay, Observatoire de Paris, Ecole Polytechnique Institut Polytechnique de Paris, ²⁴Smithsonian Astrophysical Observatory, ²⁵Princeton University, ²⁶University of Maryland at College Park, ²⁷Peking University, ²⁸University of Alaska Fairbanks

Synopsis:

Collisionless shocks are fundamental processes that are ubiquitous in space plasma physics throughout the Heliosphere and most astrophysical environments. Earth's bow shock and interplanetary shocks at 1 AU offer the most readily accessible opportunities to advance our understanding of the nature of collisionless shocks via fully-instrumented, in situ observations. One major outstanding question pertains to the energy budget of collisionless shocks, particularly how exactly collisionless shocks convert incident kinetic bulk flow energy into thermalization (heating), suprathermal particle acceleration, and a variety of plasma waves, including nonlinear structures. Furthermore, it remains unknown how those energy conversion processes change for different shock orientations (e.g., quasi-parallel vs. quasi-perpendicular) and driving conditions (upstream Alfvénic and fast Mach numbers, plasma beta, etc.). Required to address these questions are multipoint observations enabling direct measurement of the necessary plasmas, energetic particles, and electric and magnetic fields and waves, all simultaneously from upstream, downstream, and at the shock transition layer with observatory separations at ion to magnetohydrodynamic (MHD) scales. Such a configuration of spacecraft with specifically-designed instruments has never been available, and this white paper describes a conceptual mission design – MAKOS – to address these outstanding questions and advance our knowledge of the nature of collisionless shocks.

1. Scientific Motivation

Collisionless shocks are a fundamental plasma process. In astrophysical plasmas, shocks are responsible for converting kinetic bulk flow energy into plasma heat, enthalpy, plus nonthermal features, acceleration of suprathermal particles, and the excitation of a variety of linear to nonlinear plasma waves and kinetic structures. Understanding collisionless shocks is vital to the understanding of our plasma universe, from the heating and deflection of bulk flows to the acceleration of cosmic rays. Moreover, collisionless shocks directly influence our own terrestrial space environment, e.g., the bow shock's role in solar wind – magnetosphere interactions and space weather in Earth's magnetosphere-ionosphere-thermosphere system.

Despite that importance, plus decades of observations and theoretical/simulation studies, the basic ability to predict how a shock with given upstream parameters will partition the incident energy amongst the various degrees of freedom available remains elusive. Moreover, the various kinetic processes that perform that energy conversion within the shock remain impossible to resolve or only partially resolvable in prior and current observations. Goodrich et al.^[1] lays out the questions that need to be answered to enlighten us, including the reasons why existing and previous missions and datasets cannot provide a complete answer.

The heliophysics community recognizes the importance of fundamental processes through the support of the previously-launched Magnetospheric Multiscale (MMS) mission (studying the fundamental process of magnetic reconnection) and the recently-selected Helioswarm mission (studying the fundamental process of turbulence). In order to achieve a complete view of the fundamental physics that dominate our universe, collisionless shocks must also be considered a subject of the highest significance in heliophysics. This can and must be done by supporting targeted and focused opportunities to observe the terrestrial bow shock in-situ, as detailed in the mission concept for the **Multipoint Assessment of the Kinematics of Shocks (MAKOS)** mission.

We propose the Decadal Survey Steering Committee consider highlighting the implementation of the **MAKOS** mission, which is specifically designed to study a significant parameter range of collisionless shocks. The MAKOS mission is a four-satellite mission designed to target the terrestrial bow shock, with the capabilities of also observing interplanetary shocks. MAKOS must be executed to address critical questions surrounding collisionless shocks. These questions are:

- 1) *What is the partition of energy across collisionless shocks?*
- 2) *What are the processes governing energy conversion at and within collisionless shocks?*
- 3) *How and why do these processes vary with macroscopic shock parameters?*

Exhibit 1 shows an abridged version of the MAKOS Science Traceability Matrix with the mapping to the science questions listed above. The following sections summarize the MAKOS mission design, instrumentation suite, cost/risk analysis, and enhancing technological developments.

2. Investigation Description

2.1 Mission Overview

The baseline MAKOS mission concept (CML 4) comprises four spacecraft (S/C) with varying spatial separations at ion-kinetic to MHD scales in high-altitude, slightly elliptical (23.1×18.0 R_E) five-to-one (5:1) lunar resonance orbits (LROs) with oppositely oriented lines of apsides that maximize the number of bow shock crossings, even when apogee is on the nightside. Each of the two orbits has two S/C with separations on the order of ~ 100 to ~ 1000 km to obtain the required simultaneous upstream, downstream, and transition layer observations at shocks, including multipoint observations at ion-kinetic scales through every shock transition layer crossing. The separations between the S/C on the different orbits range from ~ 5 to $12 R_E$. This provides year-round crossings of the bow shock with simultaneous multipoint separations ranging from ion

MAKOS Science Traceability Matrix					Instrument Requirements			
Science Questions	Science Objectives	Physical Parameters	Observable Quantities	Instrument	Instrument & Parameter		Exp. Data Volume per Orbit	
						Measurement Req.		
[Q1] What is the energy budget both upstream and downstream of a collisionless shock?	Quantify the contribution of proton and electron thermal and kinetic energy to the shock energy budget	Simultaneous upstream and downstream moments (density, velocity, pressure, heat flux) of particle sub-populations	Simultaneous upstream and downstream core 3D velocity distribution functions	SWI	SWI	Energy Range 300 eV – 7 keV Energy Resolution 10% FOV 40° x 40° Angular Resolution 6° Temporal Resolution 0.1 s	27 GB	
				SWE				
				STI				
	Quantify the contribution of He and the CNO group thermal and kinetic energy to the shock energy budget		Simultaneous upstream and downstream suprathermal 3D velocity distribution functions	STE	SWE	Energy Range 3 eV – 1.5 keV Energy Resolution 10% Angular Coverage 4π-ster Angular Resolution 20° Temporal Resolution 0.01 s	314 GB	
				EP				
				STI				
Quantify the contribution of Poynting flux to the shock energy budget	Electric and Magnetic field contribution to the Poynting flux	Simultaneous upstream and downstream 3D DC- and AC-coupled electric and magnetic field	EFI	STE	Energy Range 500 eV – 30 keV Energy Resolution 20% Angular Coverage 4π-ster Angular Resolution 20° Temporal Resolution 1 s	102 GB		
[Q2] What are the processes governing energy conversion at and within collisionless shocks?	Particle heating	Simultaneous upstream, within shock, and downstream core, suprathermal and energetic particle 3D Velocity Distribution Functions (VDFs)	FGM					
			SCM					
			SWI					
[Q3] How and why do these processes vary with shock orientation and driving conditions?	Characterize the coherent and incoherent heating and acceleration of particle populations upstream, downstream, and within the shock front	Non-Maxwellian features responsible for observed instabilities	Simultaneous upstream, within shock, and downstream core 3D VDFs	SWE	EP	Energy Range 20 keV–10 MeV Energy Resolution 20% Species H, He, C, O, Ne, e FOV 180° Angular Resolution 30° Temporal Resolution 1 s	30 GB	
				STI				
				STE				
	Identify electric and magnetic field variations together with targeted local plasma instabilities and resulting waves within the shock		Magnetic and electric field topology and wave modes	Simultaneous upstream, within shock, and downstream 3D DC- and AC-coupled magnetic and electric field	SWI	FGM	(DC) Dynamic Range ±500 nT Resolution 10 pT Temporal Resolution 0.03125 s	278 MB
					SWE			
					STI			
Parameterize shock crossings according to the macroscopic, Rankine-Hugoniot relations	Particle-dependent macroscopic shock parameters.	Upstream, within shock, and downstream particle moments and 3D DC-coupled magnetic field	SCM	SCM	(AC) Dynamic Range ±50 nT Resolution 0.1 pT Temporal Resolution 0.001 s	12 GB		
			EFI					
			All					
Tabulate and sort observed shock crossings according to the macroscopic shock parameters for statistical analysis of science objectives	Statistical parameterization of the processes in [Q1] & [Q2] versus calculated shock parameters			All	EFI	(DC) Range ±1000 mV/m Dimensions 3 Resolution 1 mV/m Temporal Resolution 0.5 s	115 GB	
				All				
						(AC) Range ±2000 mV/m Dimensions 3 Resolution 1 mV/m Temporal Resolution 0.001 s		

Exhibit 1. MAKOS will address outstanding questions regarding the cross-scale physical processes at play at collisionless shocks.

kinetic (100~1000 km; each pair) to MHD (several R_E ; the pair of pairs) scales, as well as prolonged dwell time throughout the year in the solar wind, enabling opportunities to also study interplanetary (IP) shocks and for MAKOS to simultaneously probe electron- and ion-kinetic plus MHD-scale processes during every single bow shock and IP shock crossing (>1000 expected during MAKOS' 2-year prime mission).

MAKOS requires each S/C to carry a comprehensive science payload of particles, fields, and waves instruments specifically tailored to measure the in-situ processes at play in collisionless shocks. The need to resolve microphysical phenomena in and around each shock and to fully characterize the plasma populations upstream and downstream of each shock drives a mission requirement that the complete three-dimensional thermal and suprathermal electron and ion velocity distributions be sampled at very high temporal resolution (<1 s). This is achieved in the notional mission design by carrying multiple dedicated sensors targeting each species and energy range on a rapidly-spinning (10 RPM baseline) S/C. Furthermore, the need to resolve the evolution of the solar wind ion beam necessitates a dedicated detector that is constantly pointed into the solar wind - i.e., along a S/C spin vector anti-aligned with the solar wind flow direction.

2.2 Science Payload

The resource demands of the MAKOS science payload are summarized in Exhibit 2.

Solar Wind Ions (SWI). Two SWI sensor heads - based on the Parker Solar Probe/SWEAP/SPAN-I instrument^{[2]-[3]} - will be oriented such that their fan-like, planar (40°x~6°) fields-of-view (FOVs) are orthogonal to each other and both parallel to the nominal solar wind direction, i.e., roughly parallel to the S/C spin axis.

Instrument	#	CBE per unit (kg)	CBE Total (kg)	CBE per unit (W)	CBE Total (W)
SWI	2	3.5	7.0	3.5	7.0
SWE	4	2.6	10.4	3.2	12.8
STI	4	11.4	45.6	12.0	48.0
STE	4	2.6	10.4	3.2	12.8
EP	1	3.9	3.9	3.8	3.8
FGM	2	0.7	1.4	4.0	8.0
SCM	1	0.8	0.8	1.0	1.0
EF	1	22.0	22.0	8.4	8.4
Totals			101.5		101.8

Exhibit 2. MAKOS carries a high-TRL (≥ 6) payload specifically tailored to measure the electromagnetic fields and particle populations required to understand energy partitioning and conversion processes at collisionless shocks.

axis) – i.e., only half the EESA-H azimuthal range - pointing radially outward at $\sim 90^\circ$ spacing around the S/C to achieve the 4π -sr sky coverage and temporal resolution required for MAKOS.

Energetic Particles (EP). Each MAKOS S/C will carry a single EP sensor - based on the time-of-flight-by-total energy PSP/IS \odot IS/EPI-Lo instrument^{[6]-[7]} - with a nearly 2π -sr FOV.

Fluxgate Magnetometer (FGM). Two FGM sensors - based on the MMS/FIELDS/FGM tri-axial (orthogonal to within $\sim 1^\circ$), fluxgate instrument^{[8]-[9]} - will be mounted on a common 5-m, single-hinged boom in a “gradiometer” configuration to characterize and eliminate S/C signals of electromagnetic interference. It is assumed that the main MAKOS/FGM electronics will be housed in a common “fields” electronics box housing along with those of the SCM and EF instruments.

Search Coil Magnetometer (SCM). The three-axis SCM sensor - based on three orthogonal (to within $\sim 1^\circ$) instances of the search coil magnetometer of the Juno/WAVES instrument^[10] - will be mounted on a second 5-m, single-hinged boom (identical but oppositely mounted from the FGM boom). The MAKOS/SCM electronics will also be housed in the common “fields” electronics box.

Electric Fields (EF). The three-axis EF instrument - based on the MMS/FIELDS/ADP (axial) and SPD (spin-plane) instruments^{[9][11][12]} - will comprise twelve spherical voltage probes mounted on four 50-m wire booms in the spin-plane of the S/C and two 10-m stacer booms along its spin-axis (i.e., axial). EF will employ two probes (as implemented on the FAST mission^[13]) - separated by ten meters - on each boom to accurately resolve wave phenomena with wavelengths 100 m.

2.3 MAKOS Spacecraft Reference Design

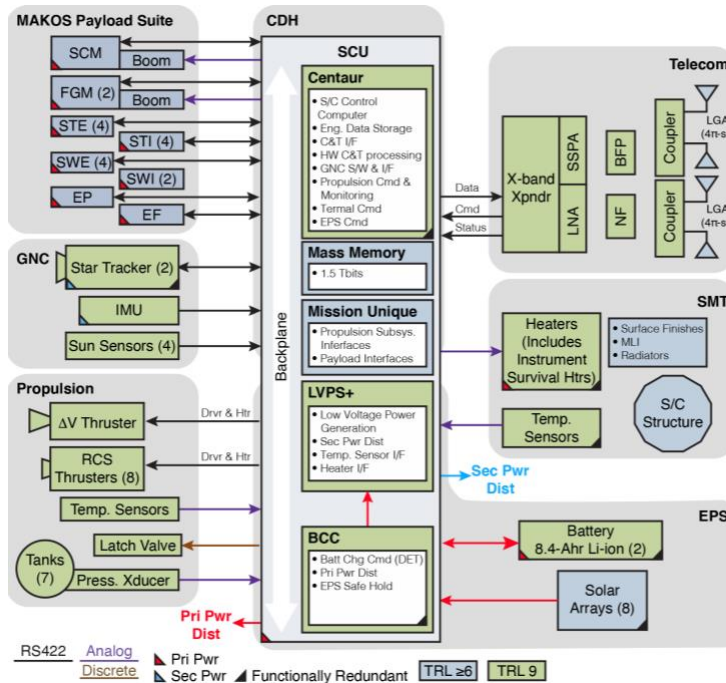
The MAKOS observatories comprise the MAKOS payload (Section 2.2) integrated with a spin-stabilized S/C using a single-string hardware architecture with functional and selective redundancy included for critical areas. The architectural approach achieves a mission success of $>90\%$ over its two-year mission lifetime as demonstrated by the NASA CYGNSS eight-observatory mission^[14], which has operated for over five years without failure.

The simple operational nature of the MAKOS instruments and science profile allows significant autonomous on-board control of the observatory during all normal science and communication operations without need for daily on-board command sequences. Observatory initialization and science operations use five sub-modes: rate damping, nutation damping, Sun acquisition/precession control, spin-rate control, and science. After initial damping of launch

Solar Wind Electrons (SWE). Four SWE detector heads - based on the WIND/3DP/EESA-L sensor^[4] - will each view the sky with a fan-like $>180^\circ \times 3^\circ$ FOV (coplanar with S/C spin axis) pointing outward at $\sim 90^\circ$ spacing around the S/C.

Suprathermal Ions (STI). Four STI detector heads - based on the STEREO/PLASTIC instrument^[5] - will each view the sky with a fan-like $\sim 180^\circ \times 6^\circ$ FOV (coplanar with the S/C spin axis) pointing radially outward at $\sim 90^\circ$ spacing around the S/C to achieve the 4π -sr sky coverage and temporal resolution required for MAKOS.

Suprathermal Electrons (STE). Four STE detector heads - based on the Wind/3DP/EESA-H instrument^[4] - will each view the sky with a fan-like $\sim 180^\circ \times 14^\circ$ FOV (coplanar with the S/C spin



S/C Functional and Selective Redundancy

- Dual fault tolerant separation sense for initial power on
- Battery cell bypass diodes
- DET channels mapped to S/A strings allows loss of S/A string
- Backup H/W and S/W timers to ensure transmitters are powered off after communication passes have completed
- Heater and temperature sensor overlay to enable functional redundancy
- Propulsion functional redundancy
- Dual star trackers
- 4π-sr Sun sensors (Safe Mode)
- 3 copies of S/C FSW are stored in MRAM and use cyclic boot tree that terminates into a “gold copy” FSW stored in write-protected boot storage
- H/W only “L0” command & telemetry capability for S/C recover if FSW fails

Exhibit 3. The MAKOS observatory reference design uses a single-string architecture with functional redundancy with heritage from the NASA CYGNSS mission.

vehicle separation rates is complete, the observatory transitions to Sun acquisition using Sun sensors and a sky-searching algorithm to locate the Sun vector. The observatory then uses reaction control thrusters to point the S/C solar arrays at the Sun using the rate and Sun sensors. The star trackers are initialized followed by spin-up of the S/C to its operational spin rate of 10 rpm. The vehicle spin axis then precesses to align with the local solar wind vector for science operations.

The MAKOS observatory design (Exhibit 3) is mission-specific to meet science requirements and instrument accommodations. Physical accommodation of the MAKOS instruments and spin stabilization implementation drives the observatory’s structure and thermal design. Fixed solar

Parameter/Item	Performance	Parameter/Item	Performance
Structure	Type	CFRP panels with milled Al supports	
	Size	Octagonal; 2.0m x 0.65m	
	1 st Mode	>210 Hz	
	SV Mass (dry)	315.7 kg	
Thermal	Architecture	Cold bias	
	Control	Heaters, MLI, radiators	
Solar Array	Configuration	6-panel, body mounted	
	Size	0.84m ²	
	Cell Type	Triple junction with AR coating	
	Cell Efficiency	28.4% (EOL)	
	Full power output	283 W (EOL)	
Battery	Configuration	8 cells/10 strings (8p10s) (x2)	
	Cell type	Li-ion	
	Capacity	56 Ahr	
	DOD during full eclipse periods	<49% with no operational restrictions	
Power	Average Load	149.5 W (cold case)	
	Margin	90%	
Space to Ground Communications	Uplink	X-band 256 kbps	
	Data Downlink	Science: 4 Mbps Engineering: 256 kbps	
Data	Data Storage	188 GBytes	
Attitude Knowledge	Star Tracker	Dual, 20 arc-sec (1σ)	
	IMU	Bias Stability: 0.3°/hr	
	Performance	<30 arc-sec (1σ)	
Attitude Control	Architecture	Spin stabilized, 10 rpm	
	Pointing	<1.3 deg	
	Nutation	<1.6 deg (p-p)	
Orbital Knowledge	GPS position	<100 m (1σ)	
	Velocity	<10 cm/s (1σ)	
Propulsion	Type	Cold Gas (SF ₆)	
	DeltaV Thrusters	1N, Isp: 45 sec (qty 3)	
	RCS Thrusters	120mN, Isp: 45 sec (qty 8)	
	Delta-V	>160 m/s when fully loaded	
	Reaction Control	6 degrees of freedom	

Exhibit 4. The MAKOS S/C performance is more than sufficient to meet the mission’s science requirements and instrument accommodations.

arrays, located on the Sun-oriented face of the observatory provide electrical power for the S/C. The LRO enables use of a simple direct energy transfer architecture for battery charging with the batteries sized to accommodate full science operations during solar eclipse periods. Primary attitude knowledge is star tracker-based augmented with rate sensors for stability and nutation determination. Sun sensors are included for emergency operations. Observatory orientation, spin-rate and precession are all controlled using an on-board cold-gas SF₆-based reaction control subsystem. Observatory positional knowledge is based on GPS receivers augmented by on-board optical navigation during GPS outages. Communication is provided by an X-band transponder and low-gain patch antennas to provide communications without interrupting science operations. On-board timing requirements are driven by science data synchronization within the constellation relative to measurement of the solar wind and electric field waveforms. Specific S/C performance characteristics are provided in Exhibit 4. Observatory magnetic and electrostatic cleanliness is key to the MAKOS instruments meeting science Level 1 requirements. MAKOS uses mature electromagnetic requirements consistent with previous missions (e.g., MMS, Cluster, THEMIS) to develop a magnetically and electrostatically clean observatory.

Expected science data generated is 53.5 GB/orbit. Baseline on-board data storage provides 188 GB or 3.5 orbits of science data storage to allow for recovery from downlink anomalies. The baseline reference communication uses a 14 Mbps X-band RF link that, with 14% overhead for CCSDS, requires ~9.6 hr to downlink science data from 1 orbit. Significantly improved data rates would be available to reduce downlink durations and/or increase data downlink quantities if the optical communications are realized prior to MAKOS implementation (see Section 4.2).

2.4 Concept of Operations

Telemetry is a major driver of the notional MAKOS mission design as the science requires very high data rates for observatory science telemetry at and around each collisionless shock crossing. Furthermore, MAKOS should also capture the highest rate data from any interplanetary shocks encountered upstream of the bow shock. Despite this, the MAKOS concept of operations (CONOPS) (Exhibit 5) is simple by design and consists of collecting science data (telemetry) from each of the four identical observatories during the two-year prime science mission. Each observatory will record telemetry in one of two science modes: i) high-rate and ii) low-rate. Even under extreme solar wind driving conditions, the bow shock is consistently located outside of the *average* (i.e., typical) magnetopause location. Thus, the average magnetopause location offers an opportune surface to use for routine orbit-to-orbit operations and systematically toggling the MAKOS S/C between high- (i.e., along the orbit *beyond* the average magnetopause location) and low-rate (i.e., along the orbit *within* the average magnetopause location) modes. Using the average magnetopause location and the orbit predicts to schedule onboard science telemetry mode changes, each MAKOS observatory shall

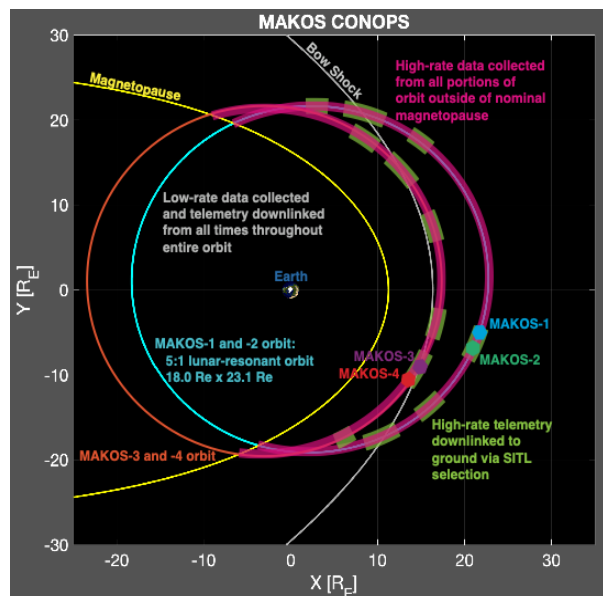


Exhibit 5. MAKOS uses two identical, 180°-phased LROs to achieve its target inter-S/C separations. A proven SITL process will be used to prioritize high-rate data obtained during predefined portions of the orbit for downlink.

switch from low- to high-rate data collection when it transits from the magnetopause into the magnetosheath (i.e., outbound model magnetopause crossings), and each observatory will switch from high- to low-rate data collection when it transits from the magnetosheath into the magnetosphere (i.e., inbound magnetopause crossings).

The MAKOS payload generates data at either 807 kbps (low-rate) or 20.875 Mbps (high-rate) to achieve the temporal resolutions required for each observable. Acquiring high-rate data only when the S/C are *sunward* of the average magnetopause requires high-rate telemetry being recorded for ~60 hrs (46%) of each 5.46-day orbit.

However, all 614 GB of science data cannot be transmitted to ground each orbit because of limitations of the communications subsystem and ground network. To ensure that all collisionless shock transits are captured during the prime mission, MAKOS will employ a “scientist-in-the-loop” (SITL) strategy similar to that used by MMS^[15]. A trained MAKOS science and data expert (i.e., SITL) will review a special low-rate data product produced onboard and telemetered to ground each orbit to make prioritized selections of which periods of the high- and low-rate data shall be telemetered to the ground. Shock crossings will be prioritized, and data from and around each shock crossing will be telemetered to the ground to ensure prime science closure. The expected SITL-selected high-rate data volume averages 5.9 GB (~1% of recorded data) per S/C per orbit; combined with the low-rate data generated each orbit (47.6 GB per S/C), this yields 53.5 GB of data to be telemetered to ground from each MAKOS S/C each orbit (9% of 595 GB total recorded data). Over the two-year prime mission, all four MAKOS S/C will telemeter 28.6 TB of total 315 TB scientific data recorded.

3 Mission Cost, Risk, and Schedule

Exhibit 6 presents a baseline cost summary estimated using multiple parametric model sets in parallel. The four-observatory configuration will require \$651M (FY22) funding as a current best estimate. Recognizing that this is a preliminary concept study, conservative reserves are applied to all cost elements: 50% for all Phase B-D work and 25% for Phase E-F. This brings the baseline estimate to \$964M (with NASA’s addition of a Phase A study and Launch Services to complete the funding). Additional development costs are not included, as baseline instruments and supporting hardware were chosen to be at TRL 6 prior to Phase A. Independent analysis by the

MAKOS Concept Study	FY22 \$M
Phase A	Not incl.
Project Management	39.8
Systems Engineering	23.4
Safety & Mission Assurance	22.9
Science / Technology	77.4
Instruments	224.1
Solar Wind Ions	15.5
Solar Wind Electrons	22.8
Suprathermal Ions	81.3
Suprathermal Electrons	35.3
Energetic Particles	13.0
Fluxgate Magnetometer	6.5
Search Coil Magnetometer	4.4
Electric Fields	29.9
Payload Electronics	15.3
Spacecraft	143.4
Mission Operations	46.4
Launch Vehicles	0.0
Ground Systems	14.1
Observatory Integration & Test	59.5
Subtotal before reserves	650.9
Reserves @ 50% B-D, 25% E-F	312.9
Total (excl. Phase A & Launch Services)	963.8

Exhibit 6. MAKOS cost by WBS.

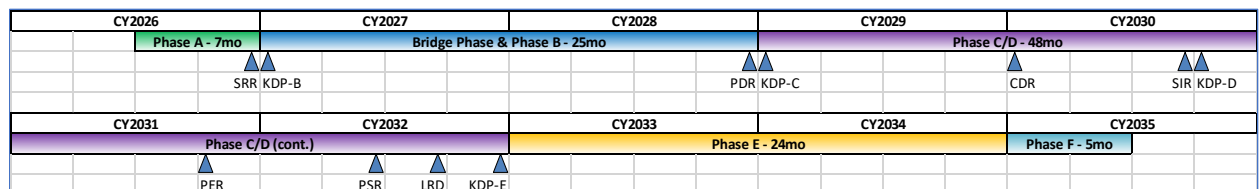


Exhibit 7. The MAKOS development plan baselines 79 months for Phases A–D, with a staggered observatory AI&T approach - including a 3-month cruise and commissioning, followed by a 2-year Phase E.

#	Risk	Type	L	C	Mitigation
1	IF a launch issue precludes all four S/C from achieving the necessary formation, THEN there could be delay to the science phase and/or impact to science closure.	Cost, Schedule	1	5	Phase A trades will consider additional propulsion capacity in S/C design to potentially enable achievement of baseline MAKOS configuration from a single launch.
2	IF instrument cross-calibration requires more analysis to resolve known challenges and ensure data product adequacy, THEN additional effort would be required.	Cost, Technical	3	2	Use of advanced data analytic techniques to develop novel ways to cross-correlate the data using timing, position, and events to improve completeness of datasets for science would be required.
3	IF specialized component updates are needed for the EF instrument deployment mechanism, THEN additional development effort would be required.	Cost, Technical	2	2	Additional design, prototyping, and testing will be conducted to reduce likelihood of failure of the EF deployment mechanism.

Exhibit 8. MAKOS has no severe mission risks and favorable mitigations for the top three identified risks. (L= risk likelihood, C= risk consequence)

NASA Goddard Cost Estimating, Modeling and Analysis (CEMA) Office concluded that the MAKOS baseline budget with proposed reserves is more than adequate to fund this project.

The MAKOS risk assessment combines with cost to identify key risks likely to drive significant variances if not managed. A four-observatory constellation, each carrying eight instruments, is within the overall experience base of the institutional partners, but the need to deliver multiple flight units raises the criticality of certain common development issues. Exhibit 7 shows the top-level schedule with major milestones. Exhibit 8 lists the top three identified risks and potential mitigations.

4 Enhancing Technology Development Needs

Instrument Development. Obtaining more comprehensive 3D particle measurements at cadences even faster (e.g., 10-ms) than recent missions (e.g., MMS and Parker Solar Probe) – without relying on a high number of sensors - will require additional instrument development for traditional top-hat ESAs or development of new particle detection systems for low-energy space plasmas. Particular emphasis is needed in two key areas: 1) parts availability, e.g., reliable high voltage optocouplers, and 2) tuning and responsiveness of the high voltage power supplies to ensure fast measurements are being taken with sufficient accuracy. At least one vendor that has provided flight parts for previous NASA missions has existing custom optocoupler designs that can fulfill even the most ambitious high-resolution MAKOS measurement cadences.

Infrastructure. While MAKOS achieves its baseline science with current RF communications infrastructure, it requires limiting high-rate data collection to only targeted portions of the orbit. Even downlinking data only when S/C are earthward of the magnetopause (i.e., ~71-hr/orbit window) requires hours per day per S/C of Deep Space Network (DSN) time. Optical communications would drastically reduce required downlink, thus enabling significantly more science data to be downlinked and reducing SITL decisions and complexity. The much higher data rates afforded by optical downlink would enhance MAKOS by significantly reducing resource competition and/or providing additional science data and reducing the need for SITL-based operations.

5 Conclusion

MAKOS is an exciting new multi-spacecraft mission – the first ever with a comprehensive payload specifically designed to address outstanding questions and advance our knowledge of the nature of collisionless shocks. Specifically, MAKOS will provide novel multipoint observations that will enable direct measurement of the necessary plasmas, energetic particles, and electric and magnetic fields and waves, all simultaneously from upstream, downstream, and at the shock transition layer with observatory separations at ion to magnetohydrodynamic (MHD) scales.

References

- [1] Goodrich et al. (2022), “The Persistent Mystery of Collisionless Shocks”, White paper submitted to the 2024 Solar and Space Physics Decadal Survey
- [2] Kasper et al. (2016), *SSR*, **204**, 131; doi: 10.1007/s11214-015-0206-3
- [3] Whittlesey et al. (2020), *ApJS*, **246**, 74; doi: 10.3847/1538-4365/ab7370
- [4] Lin et al. (1995), *SSR*, 71, 125–153, doi:10.1007/BF00751328
- [5] Galvin et al. (2008), *SSR*, **136**, 437–486, doi:10.1007/s11214-007-9296-x
- [6] McComas et al. (2016), *SSR*, doi:10.1007/s11214-014-0059-1
- [7] Hill et al. (2017), *JGR Sp Phys*, 122, doi:10.1002/2016JA022614
- [8] Russell et al. (2016), *SSR*, **199**, 189–256, doi:10.1007/s11214-014-0057-3
- [9] Torbert et al. (2016), *SSR*, **199**, 105–135, doi:10.1007/s11214-014-0109-8
- [10] Kurth et al. (2017), *SSR*, **213**, 347–392, doi:10.1007/s11214-017-0396-y
- [11] Ergun et al. (2016), *SSR*, **199**, 167–188, doi:10.1007/s11214-014-0115-x
- [12] Lindqvist et al., (2016), *SSR*, **199**, 137–165, doi:10.1007/s11214-014-0116-9
- [13] Ergun et al. (2001), *SSR*, **98**, 67–91, doi:10.1023/A:1013131708323
- [14] Rose et al. (2013), *2013 IEEE Aerospace Conference*, doi: 10.1109/AERO.2013.6497205.
- [15] Fuselier et al. (2016), *SSR*, **199**, 77–103, doi:10.1007/s11214-014-0087-x